

MESOSCOPIC-SCALE OBSERVATIONS OF SURFACE ALLOYING, SURFACE PHASE TRANSITIONS, DOMAIN COARSENING, AND 3-D ISLAND GROWTH: Pb ON Cu(100)

G. L. Kellogg and R. A. Plass
Sandia National Laboratories
Albuquerque, NM 87185-1421

RECEIVED
JUN 06 2000
OSTI

Abstract

Low energy electron microscopy (LEEM) is used to investigate the dynamics of Pb overlayer growth on Cu(100). By following changes in surface morphology during Pb deposition, the amount of Cu transported to the surface as the Pb first alloys into the surface during formation of the $c(4 \times 4)$ phase and subsequently de-alloys during conversion to the $c(2 \times 2)$ phase is measured. We find that the added coverage of Cu during alloying is consistent with the proposed model for the $c(4 \times 4)$ alloy phase, but the added coverage during de-alloying is not consistent with the accepted model for the $c(2 \times 2)$ phase. To account for the discrepancy, we propose that Cu atoms are incorporated in the $c(2 \times 2)$ structure. Island growth and step advancement during the transition from the $c(2 \times 2)$ to $c(5\sqrt{2} \times \sqrt{2})R45^\circ$ structure agrees with this model. We also use the LEEM to identify the order and temperature of the two-dimensional melting phase transitions for the three Pb/Cu(100) surface structures. Phase transitions for the $c(5\sqrt{2} \times \sqrt{2})R45^\circ$ and $c(4 \times 4)$ structures are first-order, but the $c(2 \times 2)$ transition is second order. We determine that rotational domains of the $c(5\sqrt{2} \times \sqrt{2})R45^\circ$ structure coarsen from nanometer- to micron-sized dimensions with relatively mild heating (~ 120 C), whereas coarsening of $c(4 \times 4)$ domains requires considerably higher temperatures (~ 400 C). In studies of three-dimensional island formation, we find that the islands grow asymmetrically with an orientational dependence that is directly correlated with the domain structure of the underlying $c(5\sqrt{2} \times \sqrt{2})R45^\circ$ phase.

1. Introduction

The growth of thin metal overlayers on single-crystal metal surfaces is a subject of considerable scientific and technological interest. The interplay between the thermodynamic properties of bimetallic interfaces and the kinetic behavior of individual atoms and clusters can lead to restructuring and self-assembly processes that underlie the formation of interesting mesoscopic-scale surface structures. A fundamental understanding of metal-on-metal growth is becoming increasingly more important from a practical standpoint, as materials scientists and engineers attempt to tailor thin-film materials for applications in bimetallic catalysis, thin-film magnetic devices, corrosion resistant coatings, and materials joining processes.

The system of Pb on Cu(100) is a lattice-mismatched system (bulk lattice constant of Cu = 0.36 nm, Pb = 0.45 nm) which exhibits unusual physical properties at the mesoscale. Even though Pb is much larger than Cu, when Pb is first deposited on clean Cu(100) at or above room temperature, the Pb atoms insert themselves into the Cu surface layer [1, 2]. At 0.375 monolayer Pb, an ordered surface alloy is formed in which rows of Pb atoms alternate with rows of Cu atoms [1-4]. The LEED pattern from the ordered alloy phase is $c(4 \times 4)$ [2, 3, 5]. Continued deposition of Pb produces a surprising result. Cu atoms within the alloy layer are expelled and the surface de-alloys. At 0.5 monolayer, the Pb atoms form an ordered $c(2 \times 2)$ overlayer with Pb atoms residing in every other four-fold hollow of the Cu(100) surface [1, 4-7]. The addition of more Pb causes the $c(2 \times 2)$ overlayer to compress. At 0.6 monolayer, Pb atoms still reside in four-fold hollows, but the overlayer structure contains periodic anti-phase dislocation rows to accommodate the extra atoms. The LEED pattern from this structure is $c(5\sqrt{2} \times \sqrt{2})R45^\circ$ [6, 8]. Deposition of Pb beyond 0.6 monolayer, results in three-dimensional island growth. Atomic

DISCLAIMER

This report was prepared as an account of work sponsored by an agency of the United States Government. Neither the United States Government nor any agency thereof, nor any of their employees, make any warranty, express or implied, or assumes any legal liability or responsibility for the accuracy, completeness, or usefulness of any information, apparatus, product, or process disclosed, or represents that its use would not infringe privately owned rights. Reference herein to any specific commercial product, process, or service by trade name, trademark, manufacturer, or otherwise does not necessarily constitute or imply its endorsement, recommendation, or favoring by the United States Government or any agency thereof. The views and opinions of authors expressed herein do not necessarily state or reflect those of the United States Government or any agency thereof.

DISCLAIMER

Portions of this document may be illegible in electronic image products. Images are produced from the best available original document.

models of the three ordered structures are shown in Fig. 1 along with the associated LEED patterns.

Although the static properties of the surface alloy and overlayer structures have been well studied, there are still interesting questions relating to the dynamic processes that take place as the Pb inserts itself into the surface layer during alloying and de-alloying. To address these questions we have made direct observations of the changes in surface morphology during Pb deposition on Cu(100) at various temperatures using the low energy electron microscope (LEEM). In addition, we have measured the order and transition temperature of the two-dimensional melting phase transitions for all three ordered surface structures, identified the temperatures where orientational domains of $c(4 \times 4)$ and $c(5\sqrt{2} \times \sqrt{2})R45^\circ$ phases coarsen, and discovered an interesting correlation between the shape of three-dimensional Pb islands and the domain structure of the $c(5\sqrt{2} \times \sqrt{2})R45^\circ$ overlayer upon which they grow. The results of these studies are summarized in this article. More detailed accounts of the investigations will appear in separate publications [9].

2. Experimental

The low energy electron microscope used in this study is a commercial system based on the design of Bauer [10]. The instrument is modified from its original design to include two additional ultra-high vacuum chambers: one for Auger electron spectroscopy and a second for Ne ion sputtering. Reproducibly clean Cu(100) surfaces are obtained by heating the sample to 800 C in a 3% hydrogen/argon mixture outside the vacuum chamber (to remove sulfur from the near-surface region), followed by high-temperature Ne ion sputtering in the LEEM sample preparation chamber. During sputtering, the Ne pressure is 5×10^{-5} Torr, the bombarding voltage is 1 kV, and the sample temperature is held at 800 C. After sputtering, the sample is slow cooled

to room temperature and transferred to the LEEM main chamber without exposure to air. Pb is deposited on the Cu(100) surface in the main chamber from a heated PBN crucible. The starting material is Pb wire having a purity of 99.999%. The background pressure in the system is typically in the low to mid 10^{-10} Torr range during Pb deposition. When the deposition source is turned off, the background pressure drops into the 10^{-11} Torr range. Auger electron spectroscopy is used to verify the sample cleanliness after Pb deposition. Common impurities such as S, O, and C are all below the Auger detection limit.

3. Results and Discussion

3.1 Surface alloying and de-alloying

LEEM images recorded during Pb deposition at room temperature show a gradual texturing of the surface, but no large-scale morphological changes. Morphological changes are observed by STM [2], but at a scale below the resolution of the LEEM. In contrast, when the sample is held at elevated temperatures (120-150 C) during deposition, step motion and island nucleation and growth are apparent at a length scale of tens of nanometers. Representative LEEM images from various stages of deposition are shown in Fig. 2. All the photographs in Fig. 2 are bright-field images, i.e., images produced using only electrons from the central (0,0) LEED beam. The electron energy and focussing conditions are adjusted in each set to highlight a specific phase as the surface converts from one ordered, two-dimensional structure to another.

Figures 2(a) and 2(b) are images of the surface taken as Pb is first deposited on the clean Cu(100) surface and the $c(4 \times 4)$ phase begins to appear. Prior to deposition the only features in the image are the step indicated by the arrow in Fig. 2(a) and the step bunches below it. During deposition, the step progresses outward and two-dimensional islands nucleate and grow. Three islands are present in Fig. 2(a). There is compelling evidence that both the step progression and

island growth are due to displaced Cu and not the deposited Pb itself. First, STM images from Nagl and co-workers [1] and Robert and co-workers [2] unambiguously show Pb atoms substituted into the surface layer at low Pb coverages. Second, in the same investigations, displaced Cu is seen at the steps and in small, nucleated islands. Finally, we have evidence from our LEEM studies that the islands seen in Figs. 2(a) and (b) are not made up of Pb atoms. When the sample is cooled to below room temperature and Pb is deposited, a different type of island appears. The low-temperature islands have uniformly dark contrast (not just at the perimeter). These islands convert to the type of islands seen in Figs. 2(a) and (b) when the sample is heated. We therefore conclude that the islands produced by low-temperature deposition are Pb, and those produced by deposition at elevated temperatures are Cu.

From periodic checks of the LEED pattern, we determine that the $c(4 \times 4)$ structure is not present on the surface shown in Fig. 2(a). Thus, a significant amount of Pb is incorporated into the Cu surface before an ordered alloy begins to form. The $c(4 \times 4)$ structure first appears after approximately 0.2-0.4 monolayer Cu is expelled. The $c(4 \times 4)$ structure is imaged in Fig. 2(b) as the dark areas near the step and island edges. We confirm that the dark regions correspond to the $c(4 \times 4)$ phase by obtaining separate dark-field images, i.e., images of the surface with a non-integral order diffraction beam. Video sequences recorded during deposition show that the $c(4 \times 4)$ phase first grows out from upper side of the step edges. This observation is consistent with the STM investigations mentioned above. Completion of the $c(4 \times 4)$ phase is identified when the entire surface turns dark.

According to the model shown in Fig. 1, the $c(4 \times 4)$ phase is a surface alloy in which every other row of Cu atoms is replaced by Pb atoms [2, 3]. To form this surface, it is necessary to displace of 0.5 monolayer Cu. We measure the amount of Cu added to the surface after the

c(4x4) phase is complete. This is the sum of the area of the islands and the area of the material added to the steps. We find that the amount of added Cu ranges from 0.50 to 0.56 in three separate experiments. This result is thus consistent with the STM measurements of Robert and co-workers [2] and with the proposed surface alloy structure shown in Fig. 1.

As mentioned above, the addition of more Pb to the c(4x4) surface alloy causes the surface to de-alloy resulting in a c(2x2) overlayer phase at 0.5 monolayer. LEEM images recorded during transition from the c(4x4) to c(2x2) surface structures are shown in Figs. 2(c) and 2(d). In these images the conditions are chosen such that the c(2x2) phase appears bright. The starting surface is pure c(4x4) with small islands remaining from the growth of the c(4x4) phase (not shown). The sequence of images indicates that the c(2x2) phase nucleates at the steps and proceeds out on to the terraces in both directions. It is obvious from the images shown in Figs. 2 (c) and 2(d) that the islands on the surface grow rather than shrink during the conversion. This behavior is consistent with a model in which the rows of Cu between the rows of Pb in the c(4x4) structure are expelled during deposition and replaced by Pb. The displaced Cu moves to the steps and island edges and causes them to expand outward. It is also obvious that the islands take on a square or rectangular shape indicating a low formation energy for steps along the $\langle 110 \rangle$ -type directions.

As in the case of the formation of the c(4x4) phase, a full conversion from the c(4x4) to c(2x2) phase should result in 0.5 monolayer of displaced Cu. Previous STM measurements are consistent with this expectation [2]. However, our measurements, taken with the sample at 125 C, indicate that there is only 0.23 monolayer of added material during the conversion. To account for this difference, we propose a new model for the higher temperature c(2x2) phase in which some of the Cu remains randomly alloyed in the c(2x2) overlayer structure. This model

appears to be at odds with LEED I-V analysis of Hösler and co-workers [6, 7], who propose that the $c(2 \times 2)$ structure is a pure overlayer phase. The discrepancy could be due to the different manner in which the $c(2 \times 2)$ phase is prepared in the LEED study or simply an oversight as to the possibility that such a structure might exist. Based on our measurements above and the results for conversion of the $c(2 \times 2)$ to $c(5\sqrt{2} \times \sqrt{2})R45^\circ$ phase discussed below, we are convinced that approximately 0.25 monolayer of Cu is alloyed in the $c(2 \times 2)$ phase, at least for surfaces prepared in the manner described in this study.

Representative images taken during conversion of the surface from the $c(2 \times 2)$ to $c(5\sqrt{2} \times \sqrt{2})R45^\circ$ phases at 125 C are shown in Figs. 2(e) and 2(f). The imaging conditions are adjusted such that the $c(5\sqrt{2} \times \sqrt{2})R45^\circ$ phase appears bright. Figure 2(e) shows the surface just as the $c(5\sqrt{2} \times \sqrt{2})R45^\circ$ phase begins to appear and Fig. 2(f) shows the same surface after the transition is complete. As in the other transitions, the $c(5\sqrt{2} \times \sqrt{2})R45^\circ$ phase begins at the step edges and proceeds outwards onto the terraces. Analysis of the images indicates that there is both step progression and island growth as the surface transforms. This behavior is confirming evidence that there is indeed Cu alloyed in the $c(2 \times 2)$ structure prepared by deposition at higher temperatures. If the $c(2 \times 2)$ phase were a pure overlayer phase, there would be no movement of steps or island growth. The amount of added material during the conversion from the $c(2 \times 2)$ to $c(5\sqrt{2} \times \sqrt{2})R45^\circ$ phase is approximately 0.05 monolayer, roughly consistent with the area consumed by deposited Pb to produce the $c(5\sqrt{2} \times \sqrt{2})R45^\circ$ phase.

In addition to step progression and island growth, there are also interesting line features that appear during conversion from the $c(2 \times 2)$ to $c(5\sqrt{2} \times \sqrt{2})R45^\circ$ phase. When the surface is heated to 150 C, these features re-shape into what appears to be two-dimensional Pb-covered Cu islands. This observation suggests that even more Cu is expelled during the conversion process.

Adding the line feature area to the island and step progression areas gives a total added material coverage of ~ 0.20 monolayer, accounting for all the extra Cu alloyed in the $c(2 \times 2)$ phase. We plan to carry out additional studies to confirm that the line features are indeed very narrow two-dimensional Cu islands.

3.2 Order-disorder phase transitions

All three submonolayer surface phases of Pb on Cu(100) undergo order-disorder transitions at elevated temperatures. The temperatures at which the structures disorder have been reported previously by Sanchez and coworkers [11, 12] using thermal-energy atom scattering. Their measurements indicate that all three transitions are first order with transition temperatures of 272 C, 225 C, and 217 C for the $c(4 \times 4)$, $c(2 \times 2)$, and $c(5\sqrt{2} \times \sqrt{2})R45^\circ$ phases, respectively. We investigated the thermal behavior of the phases using both LEED and bright-field LEEM. The $c(5\sqrt{2} \times \sqrt{2})R45^\circ$ phase exhibits the sharpest behavior with a first-order phase transition at 216 C. A series of bright-field LEEM images, recorded as the temperature is lowered through the transition, is shown in Fig. 3. The brighter areas correspond to the ordered phase and the darker background corresponds to the disordered phase. The ordered phase appears in a well-defined nucleation and growth process clearly indicative of a first-order transition. The bright regions grow in with two preferred growth directions. We confirm that these two directions correspond to orientational domains of the $c(5\sqrt{2} \times \sqrt{2})R45^\circ$ structure. The behavior of domains for the $c(5\sqrt{2} \times \sqrt{2})R45^\circ$ and $c(4 \times 4)$ structures are discussed further in the next section.

Our results for phase transitions of the $c(2 \times 2)$ and $c(4 \times 4)$ structures are not consistent with those of Sanchez and coworkers [11, 12]. The $c(2 \times 2)$ phase, in particular, shows no evidence for nucleation and growth of the ordered structure as the temperature is lowered through the transition. Moreover, analysis of dark-field images from the half-order LEED spots as a function

of temperature indicates that the transition takes place over a broad range of temperature between 116 C and 275 C. This behavior is more consistent with a second-order phase transition. A much sharper transition is observed when the $c(2 \times 2)$ phase is mixed with the $c(4 \times 4)$ phase. In this case the transition temperature is found to be dependent on the ratio of the two phases, but always lower than the value reported previously. It is possible that a mixed phase was examined in the earlier work, leading to the conclusion that the $c(2 \times 2)$ order-disorder transition is first order.

In the case of the $c(4 \times 4)$ structure, our observations suggest a first-order phase transition. Bright-field LEEM images clearly show a nucleation and growth process as the temperature is lowered through the transition. However, our value for the temperature of the transition (~ 240 C) is considerably lower than that reported in the thermal-energy atom scattering work [11, 12]. Preliminary measurements indicate that the transition temperature depends on whether or not the $c(4 \times 4)$ phase is complete, and whether or not the surface is subsequently annealed to coarsen the domains. More extensive measurements are required to resolve the discrepancy for the transition temperature of $c(4 \times 4)$ surface phase.

3.3 Domain coarsening

From the models shown in Fig. 1 it is evident that both the $c(4 \times 4)$ and the $c(5\sqrt{2} \times \sqrt{2})R45^\circ$ surface structures have two-fold symmetry. These two surface phases therefore have orientational domains in perpendicular directions. The dark-field imaging procedure available in the LEEM allows us to view the size of the orientational domains and how they coarsen as a function of temperature. For structures produced by Pb deposition at room temperature, we find that the domain size is smaller than the spatial resolution of our LEEM (7.5 nm). When the surface is heated, we observe that the domains increase in size for both phases, but at

significantly different temperatures. Whereas the $c(4 \times 4)$ requires temperatures of approximately 400 C (higher than the two-dimensional melting transition), domains of the $c(5\sqrt{2} \times \sqrt{2})R45^\circ$ phase coarsen at temperatures as low as 125 C. The reason for the difference is clear. The $c(4 \times 4)$ phase is a surface alloy. To change the domain structure requires rearrangement and transport of Cu as well as Pb. In contrast, the $c(5\sqrt{2} \times \sqrt{2})R45^\circ$ phase is an overlayer structure. To coarsen this phase only requires transport of Pb on the Cu surface. Real-time images recorded during domain coarsening of the $c(5\sqrt{2} \times \sqrt{2})R45^\circ$ phase indicate that the coarsening does not take place by a well-defined nucleation and growth process, but instead by a gradual separation into two domains. The ability to produce domains large enough to be observed in the LEEM proved to be very useful in studies of the correlation between the $c(5\sqrt{2} \times \sqrt{2})R45^\circ$ domain orientations and the shape of three-dimensional Pb islands as discussed in the next section.

3.4 Three-dimensional island growth

Once the $c(5\sqrt{2} \times \sqrt{2})R45^\circ$ structure is complete, additional deposition of Pb at room temperature and above results in the formation of three-dimensional Pb islands. The growth and coarsening of these islands is observable in LEEM images. A previously unexplained feature of three-dimensional island growth is the asymmetric shape of the islands. Instead of being circular, islands grown at room temperature and above are elliptical, or sometimes rectangular in shape. The long axes of the ellipses or rectangles have two preferred orientations in directions perpendicular to each other. As discussed in detail in a separate publication [9], we discovered that the shape of the three-dimensional islands is correlated with the domain structure of the underlying $c(5\sqrt{2} \times \sqrt{2})R45^\circ$ phase. Figure 4 shows three images that identify this correlation. The two levels of contrast in the background are due to the two different domain orientations. The contrast is achieved by tilting the electron beam. In Fig. 4(a) one of the two domains (darker

contrast) is dominant over the imaged area, in Fig. 4(b) the other (lighter contrast) is dominant, and in Fig. 4(c) there is a relatively equal mixture of the two. The association of the island shape with the domain structure is obvious. From the orientation of LEED patterns with dark field images of the domain structure, we found that the long axis of the three-dimensional islands is parallel to the dislocation rows.

There are several examples evident in Fig. 4 in which the three-dimensional Pb islands extend across domain boundaries of the $c(5\sqrt{2}\times\sqrt{2})R45^\circ$ structure. It is interesting that once nucleated, these islands continue to grow with the same preferred direction even when growing into a domain with the “wrong” orientation. By viewing videotapes of the growth sequences, we observe that most islands stop growing when they encounter a domain boundary, but a few continue to grow as if the boundary were not present. We currently have no explanation for this effect, but suspect that it may be possible for the growing island to locally change the underlying domain orientation as it grows. If this is true, the gain in interfacial energy in preserving the orientational relationship of the island to the substrate is sufficient to overcome the energy required to realign the dislocation rows of the $c(5\sqrt{2}\times\sqrt{2})R45^\circ$ structure.

4. Summary

The results of this study show that dynamical studies with the LEEM can provide new insights into the growth of Pb overlayers on Cu(100). The main conclusions are: (1) the amount of Cu that is transported to the surface during surface alloying is consistent with the proposed model for the $c(4\times 4)$ phase, but mass transport during de-alloying at 70-130 C is inconsistent with the proposed model for the $c(2\times 2)$ phase; (2) the discrepancy for the de-alloying process can be explained by a new model for the $c(2\times 2)$ phase in which approximately 0.25 monolayer Cu is alloyed in the Pb surface layer; (3) Cu mass transport during conversion from the $c(2\times 2)$ to the

$c(5\sqrt{2}\times\sqrt{2})R45^0$ structure is consistent with the alloyed $c(2\times 2)$ model; (4) order-disorder phase transitions are first order for the $c(5\sqrt{2}\times\sqrt{2})R45^0$ and $c(4\times 4)$ structures, but second order for the $c(2\times 2)$ structure; (5) mixed phases of $c(2\times 2)$ and $c(4\times 4)$ structures have significantly different transition temperatures than the pure phases; (6) orientational domains of the $c(4\times 4)$ structure require temperatures above 400 C to coarsen, but relatively mild temperatures (120 C) will coarsen $c(5\sqrt{2}\times\sqrt{2})R45^0$ domains; and (7) the shape of three-dimensional islands is correlated with the domain structure of the underlying $c(5\sqrt{2}\times\sqrt{2})R45^0$ Pb overlayer.

Acknowledgements

This work is supported in part by the Department of Energy, Office of Basic Energy Sciences, Division of Materials Science. Sandia National Laboratories is a multiprogram laboratory operated by Sandia Corporation, a Lockheed Martin Company, for the U. S. DOE under Contract DE-AC04-94AL85000.

References

- [1] C. Nagl, E. Platzgummer, O. Haller, M. Schmid, and P. Varga, *Surf. Sci.* **333**, 831 (1995).
- [2] S. Robert, S. Gauthier, F. Bocquet, S. Rousset, J. L. Duvault, and J. Klein, *Surf. Sci.* **350**, 136 (1996).
- [3] Y. Gauthier, W. Moritz, and W. Hosler, *Surf. Sci.* **345**, 53 (1996).
- [4] E. Platzgummer, M. Borrell, C. Nagl, M. Schmid, and P. Varga, *Surf. Sci.* **413**, 202 (1998).
- [5] J. Henrion and G. E. Rhead, *Surf. Sci.* **29**, 20 (1972).
- [6] W. Hoesler and W. Moritz, *Surf. Sci.* **117**, 196 (1982).
- [7] W. Hoesler, W. Moritz, E. Tamura, and R. Feder, *Surf. Sci.* **171**, 55 (1986).
- [8] W. Hoesler and W. Moritz, *Surf. Sci.* **175**, 63 (1986).
- [9] R. A. Plass and G. L. Kellogg, to be published

[10] E. Bauer, Rep. Prog. Phys. 57, 895 (1994).

[11] A. Sanchez and S. Ferrer, Physical Review B-Condensed Matter 39, 5778 (1989).

[12] A. Sanchez, J. Ibanez, R. Miranda, and S. Ferrer, J. Appl. Phys. 61, 1239 (1987).

Figure Captions

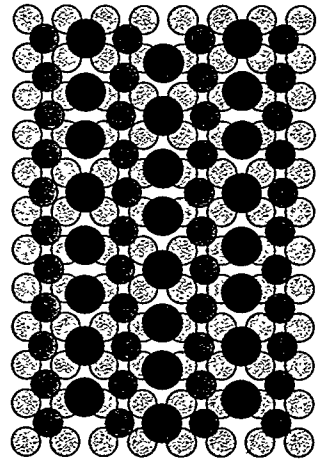
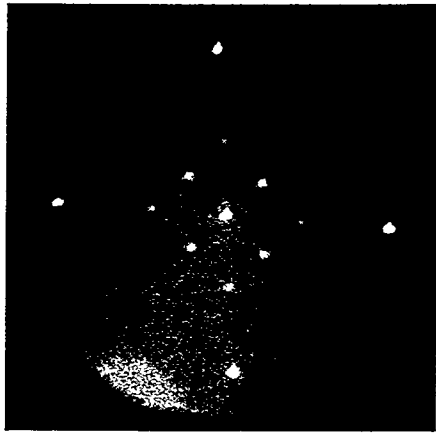
Fig. 1 (Top) LEED images from the three ordered phases of Pb on Cu(100). Pb is deposited with the sample at room temperature. The electron energy is 130 eV. (Bottom) Proposed atomic models of the three structures. Red circles represent Pb atoms, dark blue represent top-layer Cu, and light blue represent second-layer Cu.

Fig. 2 Bright-field LEEM images of a Cu(100) surfaces at various stages of Pb deposition at 125 C. (a) Cu islands nucleate and grow and steps progress as deposited Pb displaces Cu. (b) The ordered $c(4 \times 4)$ surface alloy phase appears (dark regions). (c-d) Square islands nucleate and grow during de-alloying from the $c(4 \times 4)$ to $c(2 \times 2)$ phase. (e) Islands nucleate and steps move as the surface converts from the $c(2 \times 2)$ to $c(5\sqrt{2} \times \sqrt{2})R45^\circ$ structure. (f) Line features accompany the growth of the $c(5\sqrt{2} \times \sqrt{2})R45^\circ$ phase.

Fig. 3 Bright field LEEM images showing the $c(5\sqrt{2} \times \sqrt{2})R45^\circ$ order-disorder phase transition as the temperature is lowered from above to below 216 C. The brighter areas correspond to the ordered phase and the darker background corresponds to the disordered phase.

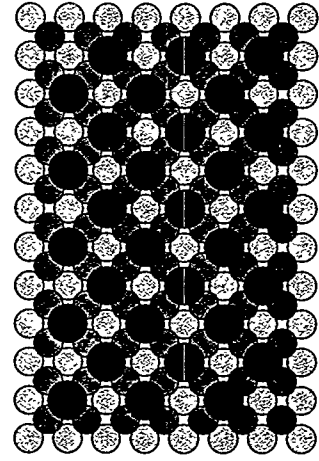
Fig. 4 Bright-field LEEM images showing the growth of three-dimensional islands (dark line segments) on the $c(5\sqrt{2} \times \sqrt{2})R45^\circ$ overlayer. The beam is tilted to identify the two orientational domains of the $c(5\sqrt{2} \times \sqrt{2})R45^\circ$ structure. The island shape is correlated with the domain structure.

(a)



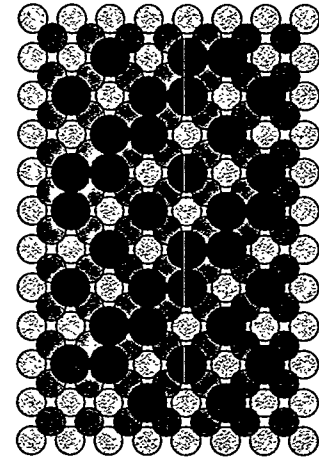
$c(4 \times 4)$ (3/8 ML)

(b)

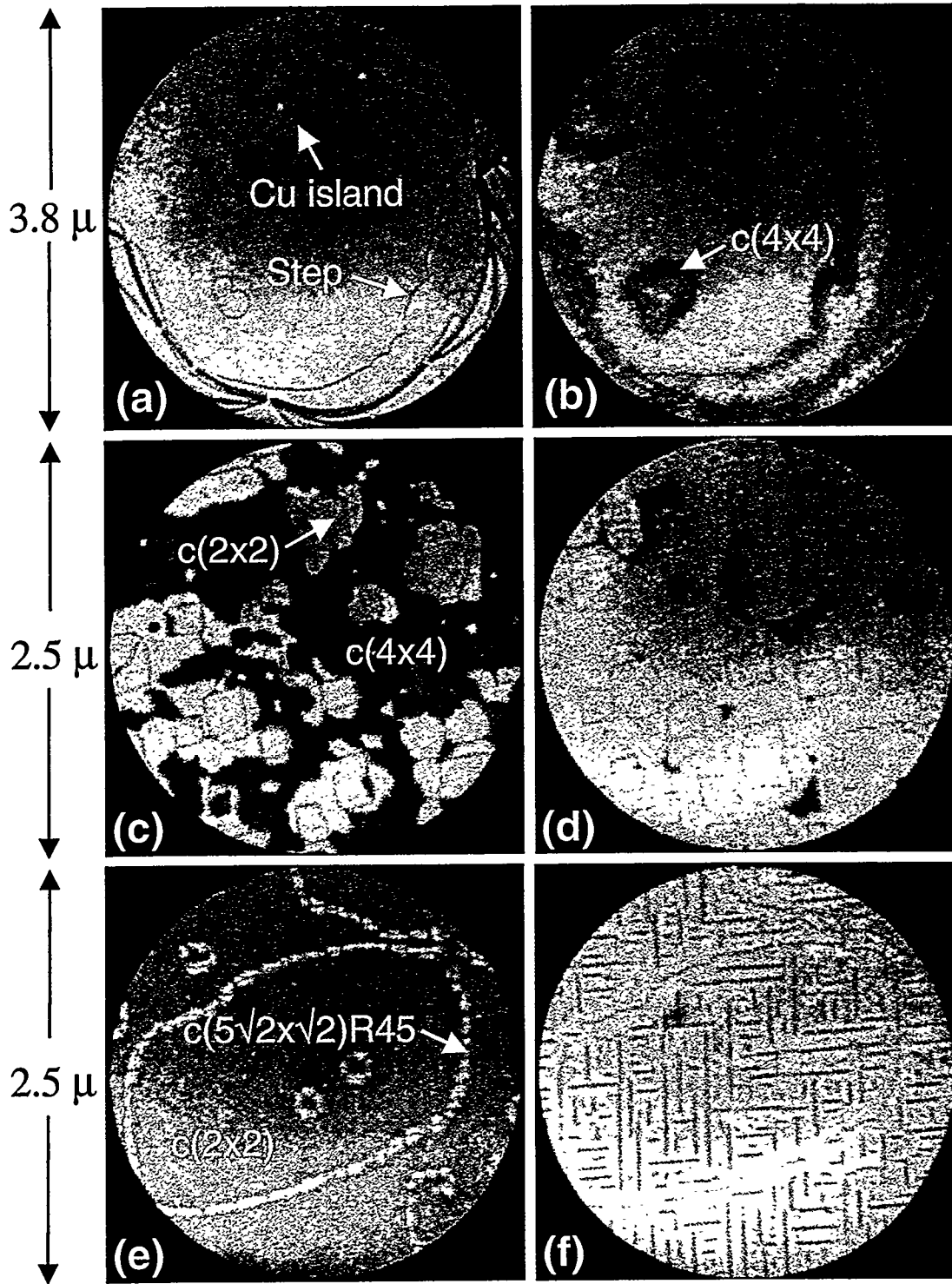


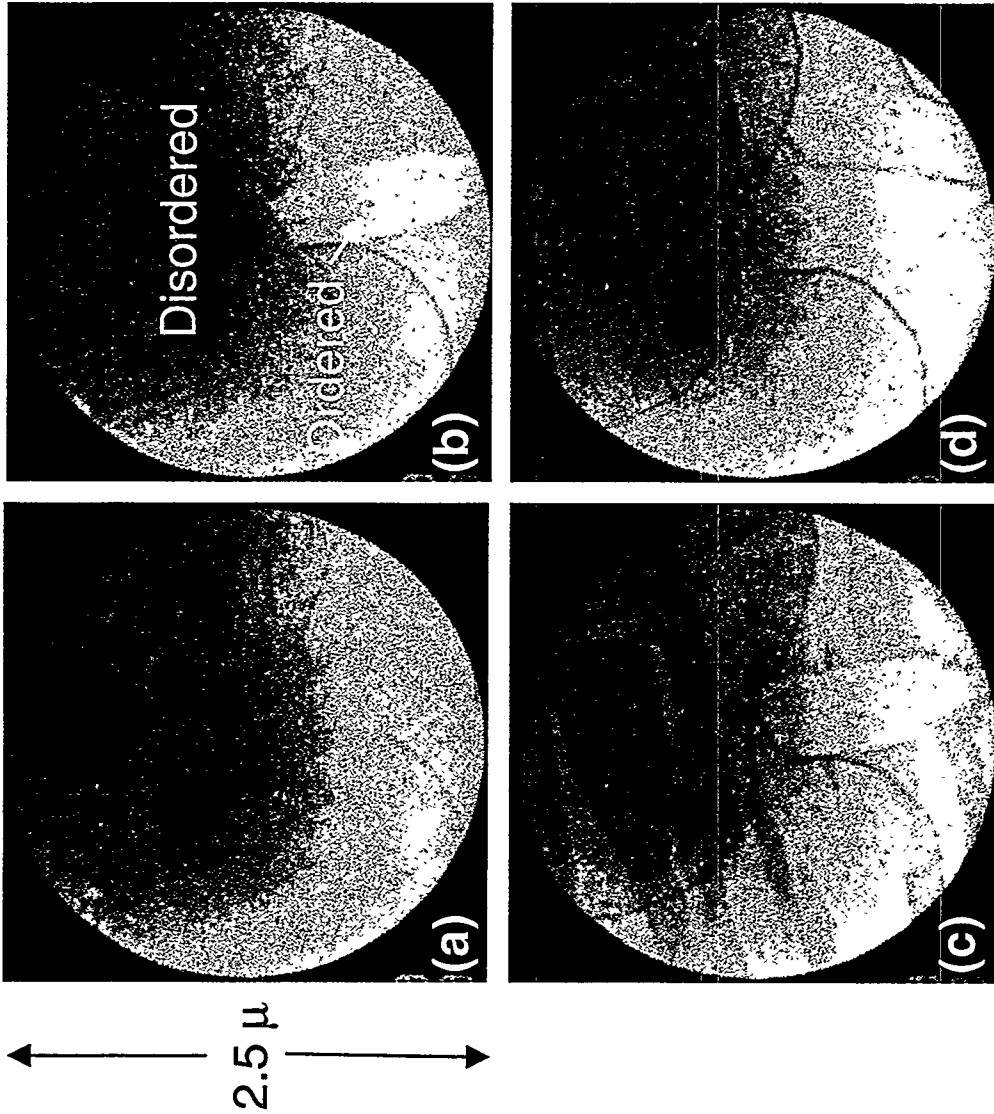
$c(2 \times 2)$ (1/2 ML)

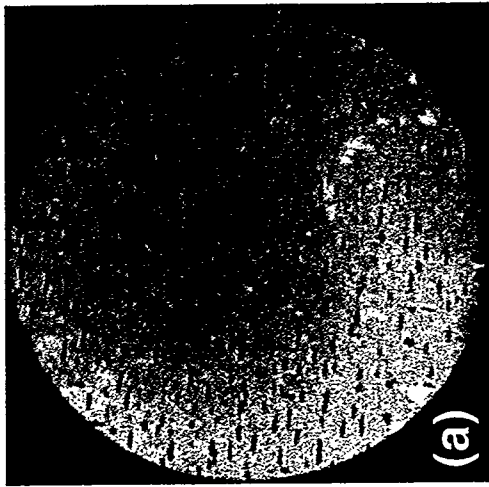
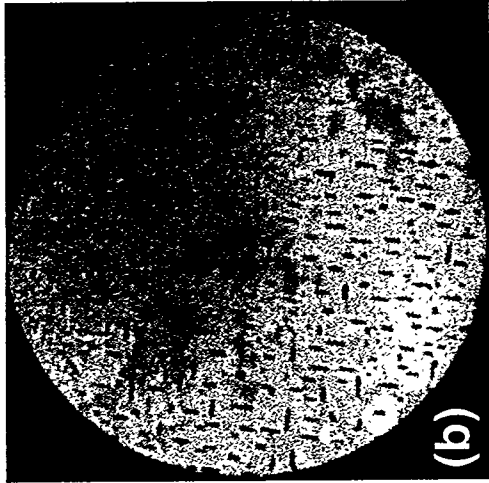
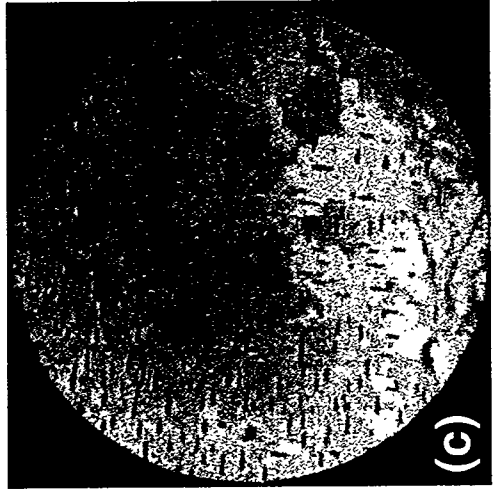
(c)



$c(5\sqrt{2} \times \sqrt{2})R45$ (6/10 ML)







10 μ